Discrete propagation and spatial solitons in nematic liquid crystals

Andrea Fratalocchi and Gaetano Assanto

Nonlinear Optics and Optoelectronics Laboratory, Italian Institute for the Physics of Matter, Università "Roma Tre," Via della Vasca Navale 84, 00146 Rome, Italy

Kasia A. Brzdąkiewicz and Mirek A. Karpierz

Faculty of Physics, Warsaw University of Technology, Koszykowa 75, 00-662 Warsaw, Poland

Received January 28, 2004

We investigate, for the first time to our knowledge, the discrete propagation of near-infrared light in a voltage-controlled array of channel waveguides in undoped nematic liquid crystals under planar anchoring conditions. This novel geometry enables us to drive the system from one-dimensional bulk diffraction to discrete propagation and, for larger excitations, to discrete spatial solitons, or nematicons. The observed phenomena are adequately described by a scalar model that encompasses the voltage-dependent reorientational response of the material.

OCIS codes: 190.4400, 190.5940, 160.3710.

Linear and nonlinear propagation of light in one-dimensional discrete systems such as optical waveguide arrays has been the subject of intense investigation, both theoretical and experimental.[1–8] Discrete solitons, reported in cubic (Kerr-like) and photorefractive media, have recently been extended to quadratic materials such as Ti-indiffused lithium niobate.[9] Remarkable results have also been achieved in one-dimensional (1D) and two-dimensional (2D) geometries achieved by photoinduced lattices through two- or four-beam interference in photorefractive crystals, respectively, facilitating propagation and localization in the transverse plane perpendicular to the direction of propagation.[10–13] Similarly to continuous systems, discrete spatial solitons originate when optically induced self-focusing balances discrete diffraction; however, in waveguide arrays it is convenient to describe the phenomenon in terms of a nonlinear response that detunes one channel with respect to the adjacent ones, thereby impeding energy transfer to the neighboring waveguides. More comprehensive descriptions include the periodic features of the whole system and address those features related to the presence of bandgaps in the dispersion of the array, particularly when a transverse velocity or a wave-front tilt is imposed on the input beam.[14] Various mechanisms that affect soliton evolution and interactions have been studied, aiming also at the demonstration of all-optical switching schemes for spatial demultiplexing, network reconfiguration, and logic.[15]

Nematic liquid crystals (NLCs) have proved to be excellent materials for nonlinear optics and its applications because of their large nonresonant nonlinearity and their extended spectral transparency. Such properties, in conjunction with the electro-optic response and a mature technology, have allowed for the demonstration of all-optical transverse localization with both coherent and partially incoherent excitation.[16–22] Through such investigations, the important role of nonlocality at milliwatt power levels in the visible and the near infrared has been emphasized.[22,23]

In this Letter we report on the experimental investigation of discrete propagation and transverse localization of light in undoped NLCs in a planar cell with an electric bias. The bias, applied through stripes of transparent indium tin oxide (ITO) electrodes, permits continuous tuning of the confinement of light from one (1D planar waveguide) to two (2D channel) transverse coordinates, in analogy to the optical definition of gratings in photorefractives.[12,13] Such voltage-controlled confinement in NLCs, at variance with solid-state arrays in semiconductors or dielectric crystals,[4,5,9] permits the engineering of this novel geometry and the precise adjustment of both the single waveguides and their coupling.

Our NLC cell is shown in Fig. 1. The top and bottom cell interfaces provide planar anchoring of the molecules of the liquid crystal 5CB in the z direction, i.e., the direction of propagation of light. A set of equally wide and periodically spaced ITO finger electrodes ($\approx$0.05 μm thick) on the top slide allows a bias to be applied across the 5-μm-thick NLC, thereby modulating the refractive-index distribution in both x and y directions through molecular reorientation in the principal plane (x, z). Since the oriented NLC is positive uniaxial, the angle $\theta = \theta(V)$ between the major

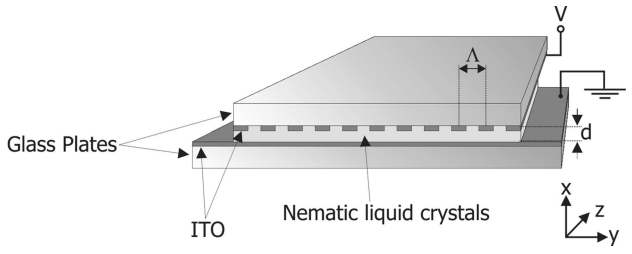

Fig. 1. Cell for the liquid-crystal waveguide array: Λ, array period; d, cell thickness; V, applied bias.

0146-9592/04/131530-03$15.00/0

molecular (optic) axis and z defines the extraordinary index: $n_e(\theta) = n_\perp n_\parallel / [n_\parallel^2 \cos^2(\theta) + n_\perp^2 \sin^2(\theta)]^{1/2}$, where $n_\perp$ and $n_\parallel$ are the indices across and along the optic axis, respectively.[24] Whereas the thin electrodes provide negligible perturbation to the planar waveguide at zero voltage, the θ-dependent increase in the transverse plane can be arranged to define an array of monomodal graded-index [$\theta = \theta(x, y)$] channel waveguides for TM polarization. From

$$K\nabla_\perp^2\theta + \frac{\Delta\epsilon_{\mathrm{RF}}E^2}{2}\sin(2\theta) = 0\,, \tag{1}$$

where K is the Frank elastic constant (taken equal for splay, bend, and twist) of the molecules and $\Delta\epsilon_{\mathrm{RF}}$ is the low-frequency anisotropy. To define the link between static electric field E and the potential V, using $\mathbf{E} = -\nabla V$, we obtain

$$\frac{\partial}{\partial x}\left[(\epsilon_\perp \cos^2\theta + \epsilon_\parallel \sin^2\theta)\frac{\partial}{\partial x}V(x,y)\right] + \epsilon_\perp \frac{\partial^2}{\partial y^2}V(x,y) = 0\,. \tag{2}$$

Equation (2) can be solved numerically to model the low-frequency response of the cell, whereas the nonlocality of the medium is accounted for by Eq. (1).

Figure 2 displays the calculated index distribution $n_e(x, y)$ for various applied voltages V. In Fig. 2(c), for $V = 1.25$ V an array of identical channels that support the (quasi-) TM_{00} mode is established. The formation of a periodic array was experimentally ascertained with cross polarizers, as shown in Fig. 3. For $V = 0$, no modulation is appreciable [Fig. 3(a)], whereas at $V = 1.4$ V the modulated intensity pattern is clearly visible [Fig. 3(b)].

While 1D diffraction takes place in the (y, z) plane when no voltage is applied, the biasing [as in Fig. 2(c)] of the sample allows for the observation of discrete diffraction. This diffraction is voltage tunable in strength through mode confinement in each channel. A 2 + 1D beam propagator with TM Gaussian excitation simulates light propagation in the structure, accounting for reorientation owing to both the bias and the light beam (of envelope A) through a version of Euler–Lagrange equation (1) that includes the nonlinear term $[\epsilon_0(n_\parallel^2 - n_\perp^2)|A|^2/4]\sin 2\theta$. Representative results are displayed in Fig. 4: Standard diffraction takes place at $V = 0$ [Fig. 4(a)], discrete diffraction is visible at low power by means of coherent coupling from input to neighboring channels at $V = 1.20$ V [Fig. 4(b)], and a discrete spatial soliton, or nematicon[25] is obtained when the excitation is intense enough to detune the input channel with respect to the adjacent channels [Fig. 4(c)]. Despite the large nonlocality encompassed by bulk NLCs[26] the anchoring conditions in our thin film reduce the lateral extent of the index perturbation, and propagation of light in the NLC's discrete array resembles the local response, as investigated in other material systems.

Experiments were carried out with a cw Nd:YAG laser oscillating at $\lambda = 1064$ nm and the light scattered above the (y, z) plane imaged with a Si:CCD camera and an optical microscope. The electrodes on the top slide, arranged in a $\Lambda = 6$ μm grating, were connected to a voltage generator at 1 kHz. An x-polarized beam was in-coupled with a waist of approximately 3 μm. Figure 5(a) is a photograph of the input light propagating in the absence of voltage, i.e., when no confinement takes place across y: the beam diffracts, becoming barely visible after a few Rayleigh ranges. In Fig. 5(b), for $V = 1.2$ V, conversely, an array of coupled 2D guides is established, and a low-power excitation of 20 mW, launched into a single channel, couples to the adjacent channels. Despite the limited coupling strength that we could achieve in this sample (without compromising the transverse confinement),

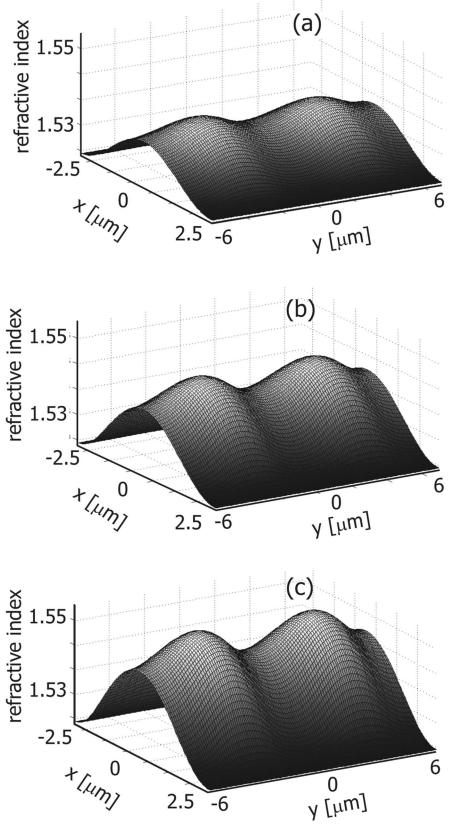

Fig. 2. Calculated refractive-index distributions versus bias: (a) $V = 1.15$ V; (b) $V = 1.20$ V; (c) $V = 1.25$ V. Liquid crystal, 5CB ($\Delta\epsilon_{\mathrm{RF}} = 12\epsilon_0$, $n_\perp = 1.6814$, $n_\parallel = 1.5158$ at 1.064 μm). Here $\Lambda = 6$ μm and $d = 5$ μm, and the covers are made from BK7 glass ($n = 1.50664$ at $\lambda = 1.064$ μm).

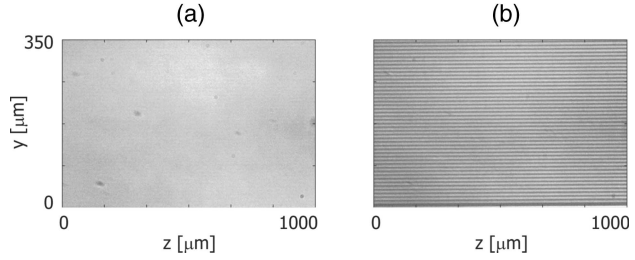

Fig. 3. Observation of induced refractive-index modulation through crossed polarizers: (a) $V = 0$ V, (b) $V = 1.4$ V.

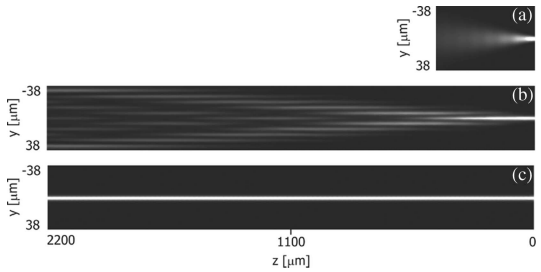

Fig. 4. Beam propagation method simulations for the NLC array (period, $\Lambda = 7\ \mu$m): (a) 1D diffraction (0.1 mW) in (y,z) in the absence of bias, (b) discrete diffraction of Gaussian input (0.1 mW) launched into one of the channels at $V = 1.20$ V, (c) a discrete nematicon for $V = 1.20$ V and 2-mW excitation.

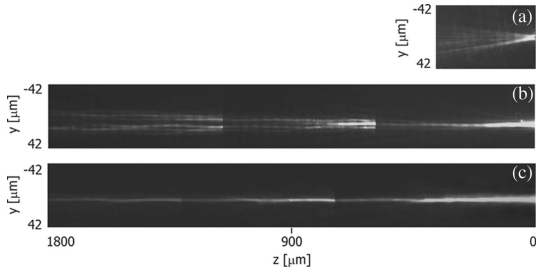

Fig. 5. Experiments with light propagation at 1064 nm: (a) 1D diffraction at $V = 0$ V, (b) low-power discrete diffraction at $V = 1.2$ V and 20-mW input, (c) discrete nematicon at $V = 1.2$ V for 35-mW input. The residual coupling and transverse–longitudinal power fluctuations shown are due partly to the limits of the camera and partly to nonuniformities in the sample.

discrete diffraction is apparent over eight channels on propagation for <2 mm. Significant propagation losses, which are due to both scattering and absorption, are also apparent in the sample. Finally, for an excitation of 35 mW we observed a discrete nematicon, as in Fig. 5(c): because of the induced mismatch, light remained localized in the input channel for propagation distances that were comparable to the absorption length ($\sim$1.25 mm in the visible).

In conclusion, we have demonstrated a novel voltage-controlled structure that, by taking advantage of both the electro-optic and the all-optical response of nematic liquid crystals, enables one to investigate the transition from bulk to discrete diffraction to discrete spatial solitons or nematicons in a waveguide array. These first experimental results are representative of a large variety of voltage-tunable configurations, which, through adjustable coupling and guided-wave confinement in a periodic array, will enable multifunctional routers and signal processors to be achieved in liquid crystals.

Partial support for this research was provided by the Italian Institute for the Physics of Matter. The authors thank M. Peccianti for enlightening discussions. G. Assanto's e-mail address is assanto@ele.uniroma3.it.

References

1. F. Lederer, S. Darmanyan, and A. Kobyakov, in *Spatial Solitons*, S. Trillo and W. Torruellas, eds. (Wiley, New York, 2002), pp. 269–292.
2. A. A. Sukhorukov, Y. S. Kivshar, H. S. Eisenberg, and Y. Silberberg, IEEE J. Quantum Electron. **39,** 31 (2003).
3. D. N. Christodoulides and R. I. Joseph, Opt. Lett. **13,** 794 (1988).
4. H. S. Eisenberg, Y. Silberberg, R. Morandotti, A. R. Boyd, and J. S. Aitchison, Phys. Rev. Lett. **81,** 3383 (1998).
5. H. S. Eisenberg, Y. Silberberg, R. Morandotti, and J. S. Aitchison, Phys. Rev. Lett. **85,** 1863 (2000).
6. F. Lederer and Y. Silberberg, Opt. Photon. News **13**(2), 49 (2002).
7. D. N. Christodoulides, F. Lederer, and Y. Silberberg, Nature **424,** 817 (2003).
8. A. C. Scott and L. MacNeil, Phys. Lett. A **98,** 87 (1983).
9. R. Schiek, R. I. Iwanow, G. I. Stegeman, T. Pertsch, F. Lederer, Y. Min, and W. Sohler, in *IEEE LEOS 2003 Annual Meeting* (Institute of Electrical and Electronics Engineers, Piscataway, N.J., 2003), postdeadline paper 1.4.
10. N. K. Efremidis, S. Sears, D. N. Christodoulides, J. W. Fleischer, and M. Segev, Phys. Rev. E **66,** 046602 (2002).
11. J. W. Fleisher, M. Segev, N. K. Efremidis, and D. N. Christodoulides, Nature **422,** 147 (2003).
12. J. W. Fleisher, T. Carmon, M. Segev, N. K. Efremidis, and D. N. Christodoulides, Phys. Rev. Lett. **90,** 023902 (2003).
13. D. Neshev, E. Ostrovskaya, Y. Kivshar, and W. Krolikowski, Opt. Lett. **28,** 710 (2003).
14. D. Mandelik, H. S. Eisenberg, Y. Silberberg, R. Morandotti, and J. S. Aitchison, Phys. Rev. Lett. **90,** 53902 (2003).
15. D. N. Christodoulides and E. D. Eugenieva, Phys. Rev. Lett. **87,** 233901 (2001).
16. E. Braun, L. P. Faucheux, and A. Libchaber, Phys. Rev. A **48,** 611 (1993).
17. M. Warenghem, J. F. Henninot, and G. Abbate, Mol. Cryst. Liq. Cryst. **320,** 207 (1998).
18. M. Karpierz, Phys. Rev. E **66,** 036603 (2002).
19. M. Peccianti, G. Assanto, A. de Luca, C. Umeton, and I. C. Khoo, Appl. Phys. Lett. **77,** 7 (2000).
20. M. Peccianti and G. Assanto, Phys. Rev. E **65,** 035603 (2002).
21. G. Assanto and M. Peccianti, IEEE J. Quantum Electron. **39,** 13 (2003).
22. M. Peccianti, C. Conti, G. Assanto, A. De Luca, and C. Umeton, J. Nonlin. Opt. Phys. Mater. **12,** 525 (2003).
23. M. Peccianti, K. A. Brzdąkiewicz, and G. Assanto, Opt. Lett. **27,** 1460 (2002).
24. D. A. Dumm, A. Fukuda, and G. R. Luckhurst, *Physical Properties of Liquid Crystals: Nematics* (INSPEC, London, 2001).
25. G. Assanto, M. Peccianti, and C. Conti, Opt. Photon. News **14**(2), 44 (2003).
26. C. Conti, M. Peccianti, and G. Assanto, Phys. Rev. Lett. **91,** 073901 (2003).